Construction and Building Materials 120 (2016) 408–417

Contents lists available at ScienceDirect

Construction and Building Materials

journal homepage: www.elsevier.com/locate/conbuildmat

Properties of cementitious mortar and concrete containing micro-encapsulated phase change materials

Amitha Jayalath [a,*], Rackel San Nicolas [a], Massoud Sofi [a], Robert Shanks [b], Tuan Ngo [a], Lu Aye [a], Priyan Mendis [a]

[a] Department of Infrastructure Engineering, The University of Melbourne, Victoria 3010, Australia
[b] School of Applied Sciences, RMIT University, VIC 3000, Australia

HIGHLIGHTS

- Microencapsulated PCM in substitution of sand increase heat capacity of concrete.
- Fineness of PCM involves a filler effect and increase cement hydration.
- Low density of PCM compared with fine aggregates reduces compressive strength.
- Microencapsulated PCM remain intact in the cementitious matrices during mixing.
- Blend of 20% v/v is proposed as optimum PCM replacement in cement-based materials.

ARTICLE INFO

Article history:
Received 5 December 2015
Received in revised form 12 May 2016
Accepted 16 May 2016
Available online 25 May 2016

Keywords:
Cement-based materials
Phase change materials
Heat capacity
Calorimetry
Thermogravimetry
Compressive strength

ABSTRACT

More efficient energy usage in buildings with increased thermal mass and better thermal insulation has attracted considerable attention in recent years. As one the most widely used construction materials in the building industry, concrete has a great potential to be converted to a high performance thermal storage material by using phase change materials (PCMs). To demonstrate this, mortar and concrete mixes were blended with microencapsulated PCM as part replacement of fine aggregates and assessed for improved thermal performance. Specimens with varying amount of microencapsulated PCM were tested using calorimetry, differential scanning calorimetry (DSC), thermogravimetry (TGA), scanning electron microscopy (SEM), compressive strength and thermal conductivity. Results show that high specific surface of microencapsulated PCM particles has induced an acceleration of the cement hydration. However, the compressive strength at 28 days is still decreased when fine aggregates were substituted by PCM. Contrary to past observations, microencapsulated PCM is observed to remain intact in the cementitious matrices and contributed significantly to improve the heat capacity as well as to reduce the thermal conductivity of the mixes tested. A blend with 20%·v/v replacement was identified as the optimum PCM replacement.

1. Introduction

Phase change materials (PCMs) store latent heat during a phase transition from solid to liquid or liquid to gas or vice versa. This latent heat can be subsequently released as thermal energy. Although sensible storage has been used for centuries for passive thermal storage, latent storage materials provide more effective storage of heat with high energy density and store heat over a narrow temperature range [1]. Research on the use of PCMs in different building materials, with various methods of incorporation has found that PCMs store significant amount of thermal energy within a building envelope with less structural mass compared with sensible heat storage [2–6]. PCMs have been used to stabilise indoor temperature in a building by reducing temperature extremes and delaying the arrival of peak temperature, therefore conserving the energy that is normally used for space conditioning [3,7]. Experimental and numerical evaluation of building thermal performance and effective thermal properties of construction materials with PCM have been reported in related studies [2,3,7].

Some researchers have analysed the innovative use of PCM in cement-based materials as a solution for improving thermal comfort and reducing energy consumed for indoor space conditioning [7–11]. Encapsulation of PCM is preferred as it can hold the liquid

* Corresponding author.
E-mail address: amithaj@student.unimelb.edu.au (A. Jayalath).

http://dx.doi.org/10.1016/j.conbuildmat.2016.05.116
0950-0618/

phase of the PCM and recent development of microencapsulated PCM has shown improved thermal properties by creating finely dispersed PCMs, with high surface area, for more efficient heat transfer. Results from a study of two full scale concrete test cells using microencapsulated PCM were presented by Cabeza et al. [7]. A lower inner temperature of 3 °C was achieved with PCM which could make considerable impact on thermal comfort levels [12]. An increase in thermal mass due to the addition of PCM was observed by a series of experiments using different amounts of PCM in concrete mixes by Hunger et al. [9]. Results showed an energy saving of 12% was achieved with 5% PCM in the mix.

While cement-based materials containing PCM have beneficial outcomes on the thermal properties of concrete, adverse consequences on mechanical properties have been reported in some studies. Hunger et al. [9] found that the addition of PCM yields lower compressive strength in concrete. Based on the reported compressive strength experimental results by Hunger et al. [9] that ranged from 75 MPa to 21 MPa, 3% PCM content in the concrete resulted in accompanying compressive strength of 35 MPa and was stated as adequate for most constructional purposes. Meshgin and Xi [10] have also reported a loss in compressive strength of concrete with addition of PCM; the mix with 20% PCM resulted in compressive strength of 15 MPa compared with 21 MPa of the control mix. Only a few studies have focused on the reasons behind the changes in mechanical properties and the reported outcomes of these studies are different to each other. Dehdezi et al. [11] stated that bursting of PCM shells under loading at a post-curing stage were the underlying reason for strength decrease. Yet the hydration effects of concrete with PCM have not been considered here. However, Hunger et al. [9] and Fernandes et al. [13] identified that PCM microcapsules tends to damage during mixing stage and leaked paraffin wax interfere with the hydration products and cause the strength reduction. Therefore further studies are needed to identify the causes of these changes in mechanical properties and the optimum amount of PCM in cement-based materials.

This research demonstrates the effect of volume fraction and dispersion of microencapsulated PCM capsules on chemical, mechanical and thermal properties in cement-based materials. A detailed experimental analysis of the mechanisms of microencapsulated PCM on cement hydration rate, strength evolution and thermal properties will be undertaken as a novel approach in identifying the optimum amount of PCM in substitution of fine aggregates that should be used under current mix design, based on the tradeoff between mechanical and thermal properties. Special emphasis is placed on cement hydration and microscopical analysis in determining the reasons for strength reduction as a basis for future developments.

2. Materials and experimental methods

2.1. Materials

The concrete mix consists of General Purpose (GP) cement, 4 mm fine aggregates (sand) and 10 mm basalt coarse aggregates. The properties of cement used are presented in Table 1. The cement type used conforms to AS3972 [14] Type GP with an estimated phase composition (by mass) of 52.13% C_3S, 19.87% C_2S, 19.64% C_3A and 2.28% C_4AF based on AS 2350.2 [15]. Finer sand compared with 4 mm fine aggregates was used for some of the mortar specimens. Sieve analysis was conducted based on AS1141.11.1 [16] for both coarse and fine aggregates. The particle size distribution for the aggregates is shown in Fig. 1. Table 2, shows the general properties of the PCM which is a paraffin based microencapsulated PCM, (Micronal DS 5040X) commercially available from BASF for the building and construction industry with a transition temperature of 23 °C. The PCM is in powder form and the particle size ranges from 50 to 300 μm. Furthermore the particle size distribution of PCM and cement was measured using laser diffraction particle size analyser, Mastersizer 3000 series.

Table 1
Chemical composition and physical properties of cement used.

Component	Amount
Calcium oxide (CaO)	66.15%
Silica (SiO_2)	20.62%
Alumina (Al_2O_3)	7.89%
Sulphur trioxide (SO_3)	2.21%
Magnesium oxide (MgO)	0.98%
Alkalis ($Na_2O + K_2O$)	0.9%
Iron oxide (Fe_2O_3)	0.75%
Titania (TiO_2)	0.32%
Phosphorus (P_2O_5)	0.18%
Loss on ignition (LOI)	2.98%
Density (g/cm^3)	3.12
Specific Area (m^2/kg)	352

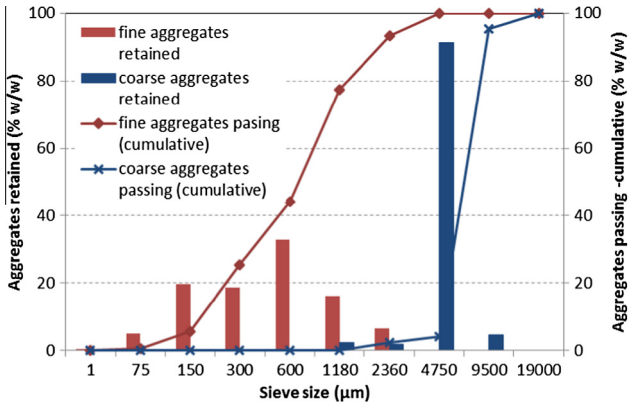

Fig. 1. Particle size distributions of fine and coarse aggregates.

Table 2
Properties of Micronal DS5040X.

Material	Transition temperature (°C)	Bulk density (kg m^{-3})	Latent heat capacity (kJ kg^{-1})
Paraffin core with Poly (methyl methacrylate) highly cross-linked shell	23	250–350	100

2.2. Experimental methods

2.2.1. Preparing concrete specimens

Concrete mixes were prepared with a fixed water-to-cement ratio of 0.5 as presented in Table 3. To provide an acceptable workability to the mixes, a third generation high water reducing superplasticiser was used. Different fractions of microencapsulated PCM ranged from 0% to 5% were used as a replacement of fine aggregates in the mix on mass basis. The mixing procedure for concrete comprised four steps. At first, all the dry ingredients except PCM were mixed for four minutes to obtain a homogenized mix. Then 90% of the total water quantity was added with the superplasticiser and mixing continued for another two minutes. Thereafter, microencapsulated PCM was added to the mixture to minimise the time of exposure to the mixing process. Finally the remaining water and superplasticiser was added to obtain a mixture with desired workability. The fresh mix was used for the subsequent

Table 3
Mix design of concrete specimens.

Sample category	PCM%	Cement (kg)	Coarse aggregates (kg)	Fine aggregates (kg)	Micronal DS5040X (kg)	Water (L)	Admixture (ml)
Control	0%	18	61.7	51.18	0.00	9.46	250
PCM 1%	1%	18	61.7	49.80	1.38	9.43	300
PCM 3%	3%	18	61.7	47.04	4.14	9.38	400
PCM 5%	5%	18	61.7	44.28	6.90	9.32	700

slump-flow test based on AS1012.3.1 [17] to measure its workability. Then cylindrical moulds measuring 100 × 200 mm and 150 × 300 mm were cast with fresh concrete in accordance with AS1012.1 [18]. All moulds were compacted using a vibrating table and then cured under laboratory conditions for 24 h. Finally, the specimens were de-moulded after 24 h and cured in water at a temperature of 23 ± 2 °C. The compressive strength tests were carried out as described in AS1012.9 [19] using Technofast compression testing machine. The average loading rate was 0.2 N/mm^2 s and three specimens from the each mix were tested at 7 and 28 days after casting.

Irrespective of the high dosage of superplasticiser, consistently lower slump was observed with increased amount of microencapsulated PCM. Moreover, due to the low density of PCM, a large difference in volume was observed between the replaced fine aggregates and the microencapsulated PCM. Thus, during mortar mixing PCM was used as a replacement of fine aggregates on volume basis and it ranged from 0% to 55% which represents 0% to 5% replacement by mass of fine aggregates.

2.2.2. Preparing mortar specimens

The same mixing procedure was followed during mixing of mortar as presented in Table 4 and cube specimens measuring 50 × 50 × 50 mm were cast for compressive strength testing in accordance with AS1012.9 [19]. All the moulds were compacted using a vibrating table and cured for 24 h under laboratory conditions. Finally they were de-moulded and cured in water at a temperature of 23 ± 2 °C until the time of testing. The compressive strength test on mortar cubes were carried out as described in AS1012.9 [19] using ELE international compression testing instrument where three specimens from the each mix were tested at 7 and 28 days after casting.

2.2.3. Calorimetry and thermogravimetry

A TAM Air isothermal calorimeter was used to measure the heat evolution of mortar paste during the hydration at constant temperature of 19 °C. For thermogravimetry (TGA), a PerkinElmer Diamond TGA/DTA was used. The mortar specimen pastes for TGA were prepared with water-to-cement ratio of 0.5 with fine sand and cured in water for 28 days at controlled temperature. At the end of the curing period the specimens were crushed into a finer powder, but the hydration process wasn't stopped with acetone as this could damage the outer polymer shell of the microencapsulated PCM. The temperature range used was 30 °C to 1000 °C in a purging N_2 environment. Initially the specimens were kept isothermally at 30 °C for 15 min and heated from 30 °C to 1000 °C at a rate of 10 K min^{-1}. Then the specimens were kept isothermally for 5 min at 1000 °C then cooled down to 30 °C with a rate of 30 K min^{-1}.

2.2.4. Differential scanning calorimetry

The specific heat of mortar specimens with different amounts of microencapsulated PCM and the melting and solidification temperature of Micronal DS5040X were measured with differential scanning calorimetry (DSC). A PerkinElmer DSC 8000 was used with a thermal cycle from 5 °C to 40 °C. Mortar specimens were crushed to powder form at an age of 28 days and small mass of about 2–4 mg was measured using a Mettler Toledo MX5 microbalance with high accuracy. The small specimen size provided good contact with aluminium specimen pans and good control of temperature throughout the specimen. The DSC instrument was initially calibrated to the onset of melting of high purity Indium standard (156.60 °C, 28.45 J g^{-1}). The heating range was 5 °C to 40 °C under a nitrogen purge (20 mL/min). Comparatively low heating/cooling rate of 2 K min^{-1} was selected to have minimum hysteresis in DSC response in different mixes [20]. The DSC scans were carried out for one complete endothermic/exothermic cycle followed by a second endothermic cycle. The results were obtained from the second endothermic cycle after deducting the base line that was carried out for an empty aluminium pan.

2.2.5. Thermal conductivity

Thermal conductivity of both concrete and mortar specimens were measured at 28 days age using two methods, namely, needle probe and C-Therm method. During casting of the specimens, a hole was made in the middle of each cylindrical specimen for the insertion of the needle probe. The specimen cylinder measured 100 × 200 mm and 50 × 110 mm for concrete and mortar respectively. All the moulds were compacted using a vibrating table and cured for 24 h under laboratory conditions. Finally they were de-moulded and cured in water for a period of 28 days at a temperature of 23 ± 2 °C. Then, the mortar specimens were heated in an oven at temperatures of between 35 °C and 40 °C until the specimen mass changed by less than 0.2 % over 24 h. This treatment was performed in an attempt to obtain a constant moisture condition of the specimens. The needle probe consisted of a manganin heater wire and a T-Type thermocouple at the centre of the tube and thermal grease was used to facilitate a better contact. All the

Table 4
Mix design of mortar specimens.

Sample category	PCM%	Cement (g)	Fine aggregates (g)	Micronal DS5040X (g)	Water (ml)	Admixture (ml)
Control	0%	450	1238.0	0	249.8	0
PCM 3%	3%	450	1200.9	5.1	249.0	0
PCM 5%	5%	450	1176.1	8.4	248.5	1
PCM 10%	10%	450	1114.2	16.9	247.3	2
PCM 15%	15%	450	1052.3	25.3	246.0	2.8
PCM 20%	20%	450	990.4	33.8	244.8	2.5
PCM 35%	35%	450	804.7	59.1	241.1	2.5
PCM 55%	55%	450	532.3	96.2	235.6	2.5

measurements were taken when the specimen temperature reached between 35 °C and 40 °C to ensure that PCM was in the liquid-state. A regulated 3 V DC and 0.85 Å was applied to the probe and the thermal conductivity was calculated by plotting temperature history vs. logarithmic time according to the standard ASTM D5334-14 [21].

Due to the non-destructive nature of C-Therm method, the same concrete and mortar specimens that were used for needle probe method were also used with the C-Therm TCi™ thermal conductivity analyser. Initially the specimen surface was polished with a sander to provide better contact with the specimen and the sensor. As in the needle probe method, specimens were heated in an oven at 35 °C–40 °C until the mass changed by less than 0.2% over 24 h. A thin layer of Wakefield type 120 thermal joint compound was used to minimise the impact of unevenness and thermal contact resistance of the surface. Initially the instrument was calibrated using ceramic standards supplied and the measurements were taken when the specimen temperature was between 35 and 40 °C to ensure that PCM is in the liquid state. The TCi sensor applies a constant current to the specimen, where there was a voltage drop in the spiral heater before and during the transient and it was used to calculate the thermal conductivity and the effusivity of the specimen.

2.2.6. Microscopical analysis

The microstructure of the pure microencapsulated PCM and the mortar specimens containing PCM was analysed using Quanta Scanning Electron Microscope (SEM) under low vacuum mode at a working distance of 10 mm. The mortar specimens from the isothermal calorimeter were removed from their glass ampoules after measuring heat of hydration and cured in water for a period of 28 days at a temperature of 23 ± 2 °C. Then a small sapecimen fragment was taken and the untouched fracture surface was observed under the SEM. To obtain a proper positioning under the microscope, the opposite side was made flat by polishing the surface with silicon discs. Backscattered electron (BSE) imaging and element mapping with energy dispersive X-ray spectroscopy (EDS) was used to analyse the microstructure and the chemical composition of the mortar specimens.

3. Results and discussion

3.1. Heat of hydration

Isothermal calorimetry was used to measure the rate of cement hydration in mortar specimens containing different amounts of PCM for 72 h. The experiments were carried out at 19 °C isothermal condition as the phase transition temperature of Micronal DS 5040X was at 23 °C and the results are presented in Fig. 2.

The plots of isothermal heat of hydration curves showed that the replacement of sand with microencapsulated PCM result in an increment and a delay in maximum rate of heat of hydration compared with the control mix. With the higher proportion of PCM in mortar specimens, a higher peak and a further delay in heat of hydration was noticed. The mix with 20% and 50% v/v replacement with PCM showed a 1 h and 2.5 h delay, respectively, compared with the control mix. The effect of dilution was not considered as there was no replacement of cement in the mix. The particle size of Micronal DS 5040X, which is in the range 50–300 μm, was small compared with 4 mm fine aggregates as shown in Fig. 1. The particle size distribution of PCM, cement and fine aggregates is presented in Fig. 3.

The cumulative particle size distribution (PSD) curves of Micronal DS5040X ranges between PSD of cement and fine aggregates. The presence of small particles in cement hydration favours heterogeneous nucleation at low energy levels where chemical activation of cement hydration is realised through physical catalyst [22]. The PCM particles falls within the smallest family of cement particles, which is less than 10 μm, provides a higher surface area and facilitate growth of hydration products. In this study the fine aggregates are replaced with comparatively smaller particles of micronised PCM. The introduction of microencapsulated PCM improves the space filling properties in the matrix and affects favourably in stimulation of cement hydration [23]. These factors stimulate the rate of hydration physically, as shown in the isothermal plots. But the arrival of maximum heat of hydration is delayed due to the latent heat of PCM.

3.2. Thermogravimetry (TGA)

Thermogravimetry on mortar specimens was carried out in order to study the effect of microencapsulated PCM on the formation of hydration products. The reaction between cement and water produces different hydration products mainly calcium silicate hydrate (C-S-H) and calcium hydroxide (CH). During the heating period of a mortar specimen, decomposition of the hydration products takes place at specific temperature ranges and the observed mass loss can be used for the quantification of hydration products. The dehydration of C-S-H and dehydroxylation of CH were observed in the range of 35 °C to 540 °C. The derivative thermogravimetry curve (DTG) provides clear identification of the temperature boundaries where different decomposition processes takes place as shown in Fig. 4.

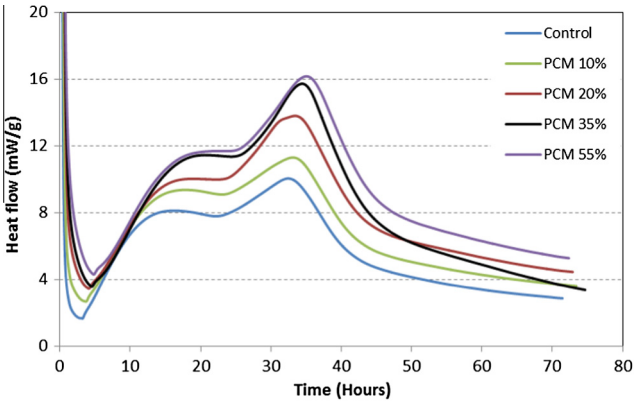

Fig. 2. The effect of microencapsulated PCM on cement hydration reaction rates with isothermal calorimetry at 19 °C.

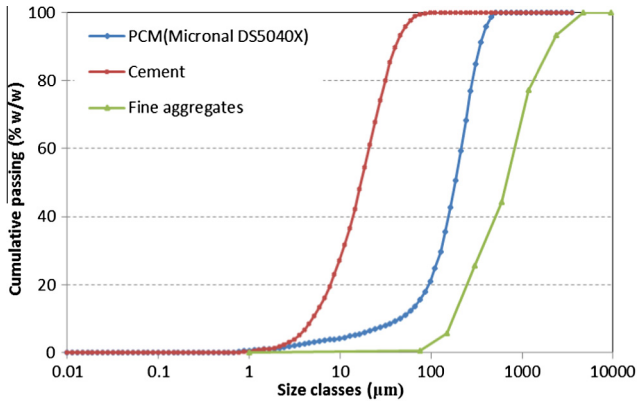

Fig. 3. Particle size distributions of PCM (Micronal DS5040X), cement and fine aggregates.

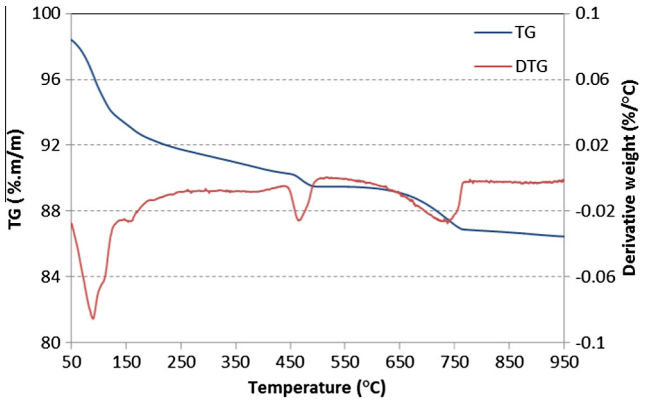

Fig. 4. TG and DTG curve of mortar specimen with 20% of microencapsulated PCM in 28 days curing time.

The weight loss observed in the range 400 °C to 540 °C represents dehydroxylation of CH. The amount of CH as a percentage of anhydrous specimen weight at 950 °C can be calculated as follows [24,25].

$$CH_1 = \frac{W_{400} - W_{540}}{W_{950}} \cdot \frac{m_{CH}}{m_{H_2O}} \quad (1)$$

where W is the specimen weight at a specified temperature. The molecular mass of CH and H_2O is represented as m_{CH} and m_{H_2O}, respectively. When the specimen is exposed to air, carbonation will take place where existing CH in the specimen reacts with CO_2 to create calcium carbonate ($C\bar{C}$). The decarbonation of $C\bar{C}$ occurs in the temperature range of 600 °C to 800 °C on the DTG curve. Thus, the corrected value for the CH content with consideration of the effect of carbonation at 600 °C and 800 °C, can be calculated as follows.

$$CH = CH_1 + \frac{m_{CH}}{m_{CaCO_3}} \cdot C\bar{C} \quad (2)$$

The total water loss for the temperature range of 35 °C to 540 °C on DTG curve was used to calculate the amount of water related to hydrated products (WH) except for CH. The degree of hydration of different mixes can be calculated using the amount of chemically bound water in the matrix [26].

$$W_n = \frac{W_{900} - W_{105}}{W_{950}} - LOI \quad (3)$$

where W_n is the chemically bound water as a percentage of anhydrous specimen weight at 950 °C; LOI is the loss of ignition of cement. The amount of chemically bound water at complete hydration $W_{n,\infty}$, varies between 0.18 and 0.26 according to [26,27] and a common value of 0.25 was used in this study. The LOI of cement at 1000 °C is used as 2.98% from literature [28]. The degree of hydration ($\propto_H$.)ased on the chemically bound water is calculated as follows.

$$\alpha_H = \frac{W_n}{W_{n,\infty}} \quad (4)$$

The DTG curves for the different mixes are presented in Fig. 5. With higher amount of microencapsulated PCM, higher weight loss was observed throughout the temperature range of 50 °C to 800 °C. It indicates that the replacement of sand with microencapsulated PCM has an influence on the CH content and the water related to hydrated products. The calculated values for CH and water content are presented in Figs. 6 and 7. However, with a higher proportion of microencapsulated PCM, higher amounts of CH and water content was observed. Due to the small particle size, PCM shows a similar

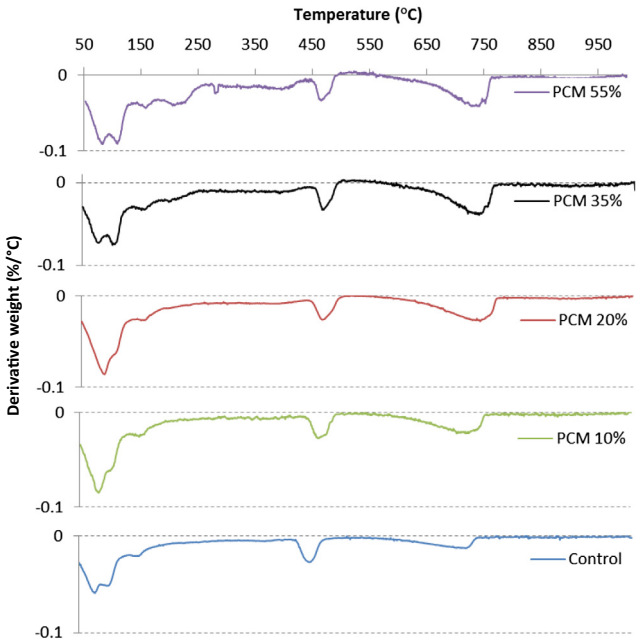

Fig. 5. DTG curve of mortar specimen; control and with10%, 20%, 35% and 55% of microencapsulated PCM in 28 days curing time.

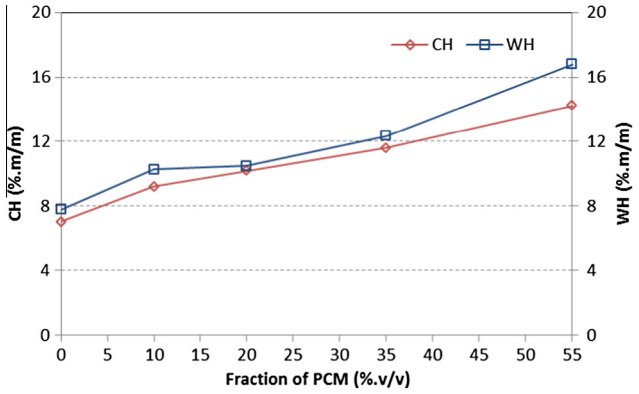

Fig. 6. The amount of calcium hydroxide and water related to hydrated products except of CH (WH) relative to PCM content.

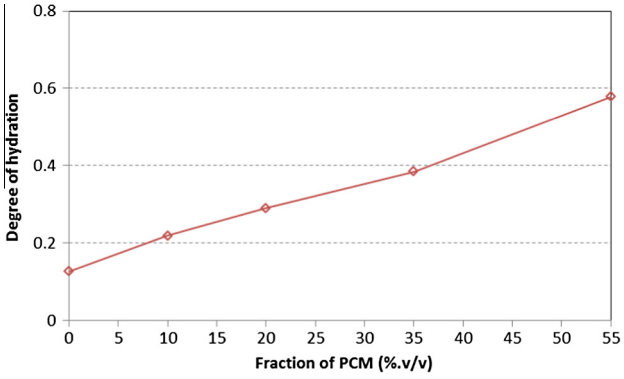

Fig. 7. Degree of hydration for mortar specimens at the age of 28 days with different PCM fractions based on TGA.

behaviour to other small supplementary materials like fly ash [25] and facilitates a filler effect in the matrix. The increased presence of micronized particles of PCM stimulates the hydration reaction

and, therefore, the CH and water contents are increased. As there is no replacement of cement with PCM, cement content for all the mixes was constant, thus the effect of dilution is neglected. The presence of nucleation sites with the addition of microencapsulated PCM was further supported by the plots on degree of hydration of the mortar specimens as discussed previously.

3.3. Compressive strength

Compressive strength development for both concrete and mortar specimens were evaluated with different proportions of microencapsulated PCM. In literature, the addition of PCM to cement-based materials yields a reduction in strength [10,11,13]. Thus, to have a better understanding of strength variation and suitable mix proportions, the number of mortar mixes was increased compared with the number of concrete mixes and ranges between 0% and 55% volume replacements of fine aggregates (sand). The volume replacement of sand from 0% to 55% in mortar mixes represents 0% and 5% mass replacement in concrete mixes due to the low density of microencapsulated PCM. The results of Fig. 8 and Fig. 9 show the effects of addition of microencapsulated PCM on the compressive strength of concrete and the mortar mixes, respectively. Overall, a reduction in strength of mortar and concrete specimens was observed. Both mortar and concrete compressive strength results showed a consistency in results and the difference in strength value of a specific mix of mortar and the respective mix of concrete can be attributed to presence of coarse aggregates in concrete.

In the different mixes studied, sand was replaced with microencapsulated PCM with two methods, either by mass or by volume, yet seems to yield the same trend for compressive strength test results except the dryness noticed during the mixing stage of concrete in mass basis. The strength reduction in 28 days is approximately 33%, 63% and 69% for 1%, 3% and 5% PCM replacement by mass, in the concrete mixes respectively. The mortar compositions show a reduction in strength at the age of 28 days in a range of 38%, 14%, 27%, 43% and 50% approximately for 5%, 10%, 20%, 35% and 55% replacement by volume, respectively.

Though the results from heat of hydration and the TGA analysis on mortar shows the presence of micronized particles of PCM accelerated the hydration reaction and increased the amount of hydration products, the compressive strength results show a loss in strength with increasing amount of PCM. With respect to all the test results obtained from heat of hydration, TGA and compressive strength test, two contradictory factors can contribute towards strength variation of these mortar specimens. First is the replacement of sand with microencapsulated PCMs. PCMs are soft particles compared with hard particles like sand, therefore the strength was reduced. Second is that the small particle size of microencapsulated PCM has increased nucleation sites for cement hydration, which should aid in strength increment. From 0% to 5% replacement by volume, the first factor is predominant, and due to a low dosage of PCMs, the number of nucleation sites is far from the optimum value. Hence a considerable amount of strength loss was observed. From 10% to 20%, the replacement of sand with soft particles has an overall effect on the strength results, thus the strength values were lower compared with the control mix. However the dosage level of microencapsulated PCM was sufficient to create an optimum level of nucleation sites, thus an increase in strength was observed compared with low dosage mixes. From 35% to 55% replacement by volume, with the high dosage level of PCM, first factor dominated the reduction of strength. Though the high volume of microencapsulated PCM should support the creation of nucleation sites, the replacement in high volumes made the mixture more linear, so the contribution of nucleation sites had less prominence in deciding the strength result. Moreover addition of microencapsulated PCM can increase the porosity of the mix, which can lead to a reduction in strength [11]. Furthermore, if the PCM particles are broken, the void space that was previously occupied by the PCM particles helps to increase the porosity of the matrix [11]. The rates between 10% and 20% replacement by volume of fine aggregates showed a comparatively lower reduction in strength compared with the other dosage levels. The average reduction in compressive strength is 24% with 10% to 20% replacement compared with 46% for 35% to 55% replacement of fine aggregates by volume. Thus it was observed that the volume replacement from 10% to 20% of sand with PCM would be the most suitable level of replacement to maintain an acceptable level of strength reduction for a range of applications in practice.

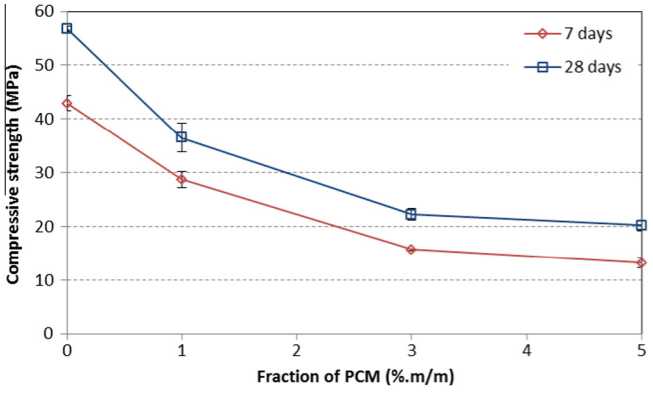

Fig. 8. The compressive strength of concrete samples at the age of 7 and 28 days with PCM replacement on mass basis.

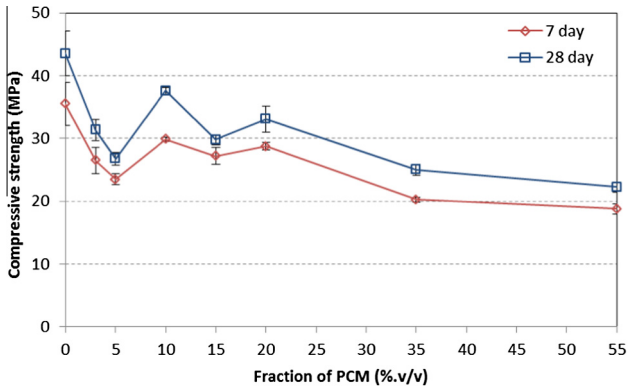

Fig. 9. The compressive strength of mortar samples at the age of 7 and 28 days with PCM replacement on volume basis.

3.4. Heat capacity

The heat capacity of mortar specimens with different amounts of microencapsulated PCM and the melting and solidification temperature of Micronal DS5040X were measured with differential scanning calorimetry (DSC). Experiments were carried out on 2–4 mg in powder form of the specimen. Due to limitation on specimen size, concrete specimens with 10 mm coarse aggregates were not used for heat capacity measurement. Thermal mass of the mortar specimens were calculated as follows and the results are presented in Fig. 12.

$$M_{TH} = m \cdot C_p \tag{5}$$

where M_{TH} is the thermal mass ($J\,K^{-1}$), m is the mass of $50 \times 50 \times 50$ mm mortar cube (kg) and the C_p is the heat capacity ($J\,kg^{-1}\,K^{-1}$).

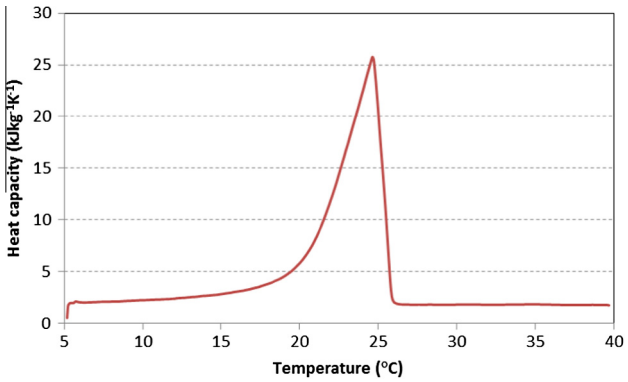

Fig. 10. DSC curves (endothermic) for pure microencapsulated PCM.

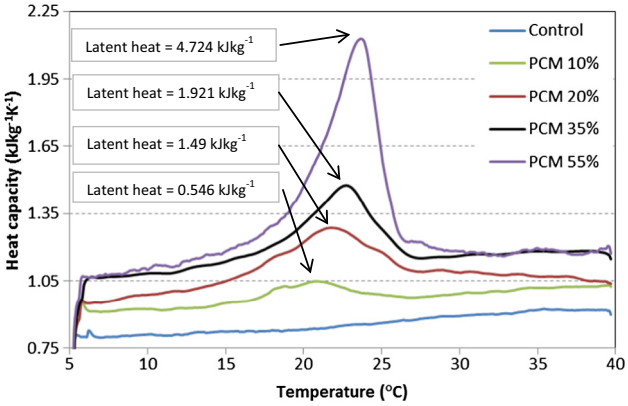

Fig. 11. DSC curves (endothermic) for mortar samples with different microencapsulated PCM proportions in 28 days of curing time.

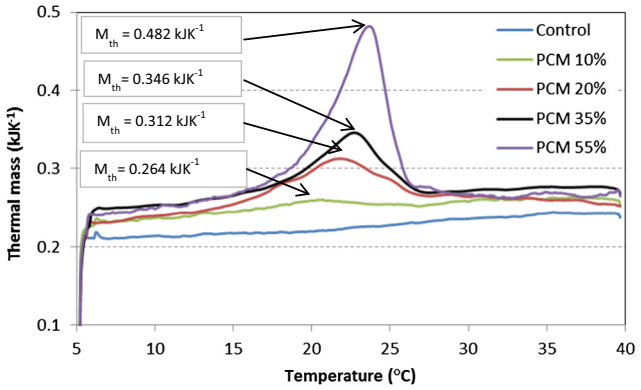

Fig. 12. Thermal mass for mortar specimens (50 × 50 × 50 mm cube) with different PCM proportions.

The DSC curves for Micronal DS5040X show an onset temperature at 20.2 °C with an endothermic peak at 24.6 °C as shown in Fig. 10. The enthalpy of phase change was measured by the area under the curve during the phase transmission. The latent heat capacity of pure microencapsulated PCM was found to be 84.69 kJ kg^{-1}.

The heat capacity and thermal mass of mortar mixes with different amount of PCM is presented in Fig. 11 and 12 respectively. The addition of PCM increases the heat capacity of the mortar specimens considerably. The latent heat capacity of 55% v/v replacement has 3 times increment compared with that of 20% v/v replacement. However the thermal mass of the 55% v/v replacement has only 1.8 times increment compared with that of the 20% v/v replacement. This was due to the reduction in density with increased microencapsulated PCM replacement in the mix and indicates a presence of an optimum amount of microencapsulated PCM in mortar with regards to thermal mass and strength properties. An increase in the peak endothermic temperature of the mortar mixes with increasing proportion of PCM was observed, as presented in Fig. 11. PCM delays the entry of heat and the increased amount of microencapsulated PCM creates a thermal gradient in the specimen. However a comparatively low heating rate of 2 K min^{-1} was used to minimise the hysteresis [20]. The peak temperature of the different mixes was within a range of ±3 °C compared with Micronal DS5040X, which showed the highest endothermic peak of 24.6 °C.

3.5. Thermal conductivity

The thermal conductivity of the concrete and mortar specimens with different proportions of microencapsulated PCM has been measured using two methods; namely, C-Therm and needle probe method. Thermal conductivity at 28 days of curing time was measured when the microencapsulated PCM is in liquid stage. The results are presented in Fig. 13 and a good relationship was noted between the two methods. A reduction in thermal conductivity with the increase of PCM amount in both concrete and mortar mixes was observed. Since the thermal conductivity of sand is high compared with microencapsulated PCM, replacement of sand has contributed towards the reduction in thermal conductivity of the mix. Also the increased amount of entrapped air, observed in literature with the addition of PCM in concrete [9], replaces some of the

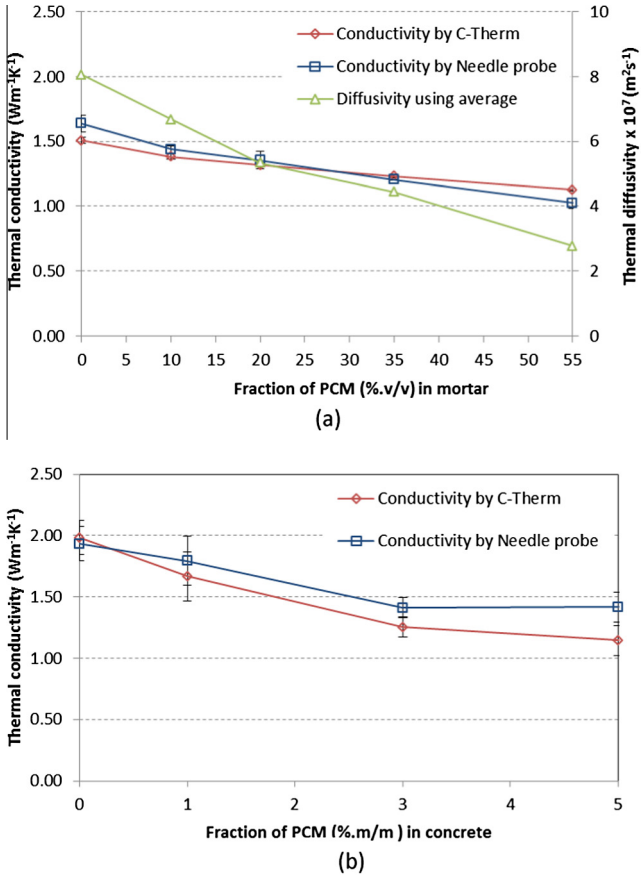

Fig. 13. (a) Thermal conductivity and thermal diffusivity of mortar, (b) thermal conductivity of concrete with C-Therm and needle probe method in 28 days.

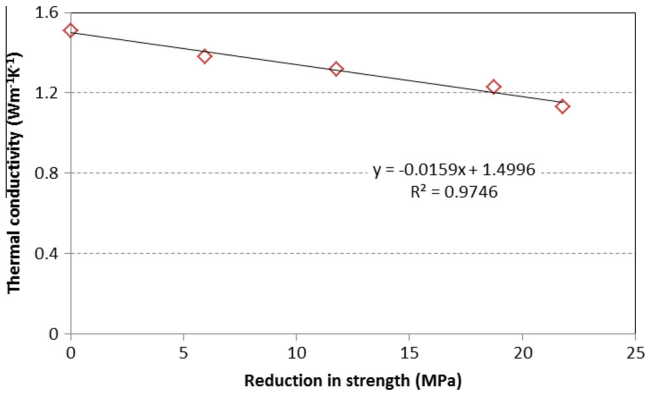

Fig. 14. The relationship between loss in compressive strength and the reduction in thermal conductivity of mortar samples with microencapsulated PCM.

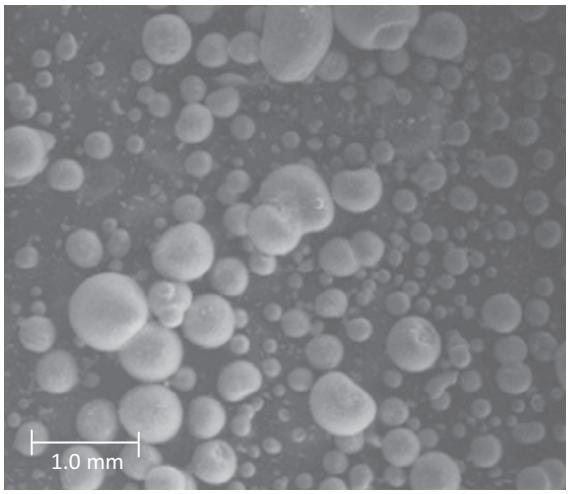

Fig. 15. SEM micrograph (using BSE detector) of Micronal DS5040X and their agglomerates.

heat transfer by conduction with natural convection, thus reduces the thermal conductivity. The thermal diffusivity ($m^2\ s^{-1}$) of mortar mixes were calculated as follows.

$$\alpha_H = k/\rho \cdot C_p \quad (6)$$

where k is the thermal conductivity ($W\ m^{-1}\ K^{-1}$) and ρ density ($kg\ m^{-3}$). Diffusivity is the ability to transfer heat relative to its ability to store heat. The addition of PCM shows a reduction in the diffusivity of mortar due to reduction in thermal conductivity and increase in the heat capacity. Materials with low diffusivity show a high thermal inertia and provide better thermal insulation properties, especially in building and construction applications. However it should be noted that the achievement of reduction in thermal conductivity along with reduction in thermal diffusivity is gained through reduction in compressive strength of the material. When the reduction of thermal conductivity of mortar is compared with the strength loss for the 0% to 55% replacement with microencapsulated PCM by volume, a close linear relationship was observed as presented in Fig. 14. For each 1 MPa drop in compressive strength, a $0.016\ Wm^{-1}\ K^{-1}$ reduction in thermal conductivity was observed for mortar.

3.6. Microscopical analysis of mortar containing microencapsulated PCM

The effect of microstructural changes on the extent of changes in the mechanical properties has also been evaluated using scanning electron microscopy (SEM) on the undisturbed fracture surface of mortar with microencapsulated PCM. The presence of some agglomerates of smaller PCM particles was observed in the BSE images of Micronal DS5040X. The microencapsulated PCM particles are spherical with a porous outer shell of polymethyl methacrylate which encapsulates the paraffin core. Fairly small amount of PCM particles were broken and the inner paraffin core was visible as shown in Fig. 15.

The BSE images of mortar specimens showed microcapsules of PCM is distributed in the matrix and well bonded with the binder. No fractures or damage was noticed around the perimeter of fine aggregates or the PCM particles, which ensures good integrity between the binder and the PCM as shown in Fig. 16(a). The PCM particles in mortar specimens were in spherical form and no deformed or crushed PCM microcapsules were noticed in almost all the mixes.

Some previous studies suggest that PCM particles could be broken during the mixing process and the released paraffin can interfere with the hydration products [9]. The spherical nature of the PCM microcapsules confirmed by the outer perimeter of the capsule suggests that these microcapsules were not damaged during mixing and the damage has occurred during post-curing stage. As the observed plane was an undisturbed fracture plane of the mortar specimen, clear evidence of cut-off PCM particles was noticed on the fracture plane of the specimen, as shown in Fig. 16(b). Some of the collapsed polymer shell and paraffin nodules were noticed inside some of the spherical voids. This damage could be due to the loading, where some evidence of fracture

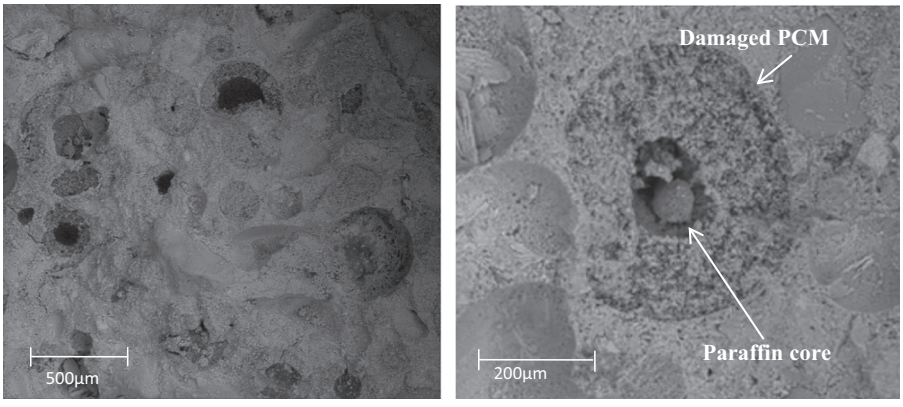

Fig. 16. SEM micrograph (using BSE detector) of (a) mortar fracture surface with microencapsulated PCM, (b) broken PCM particle.

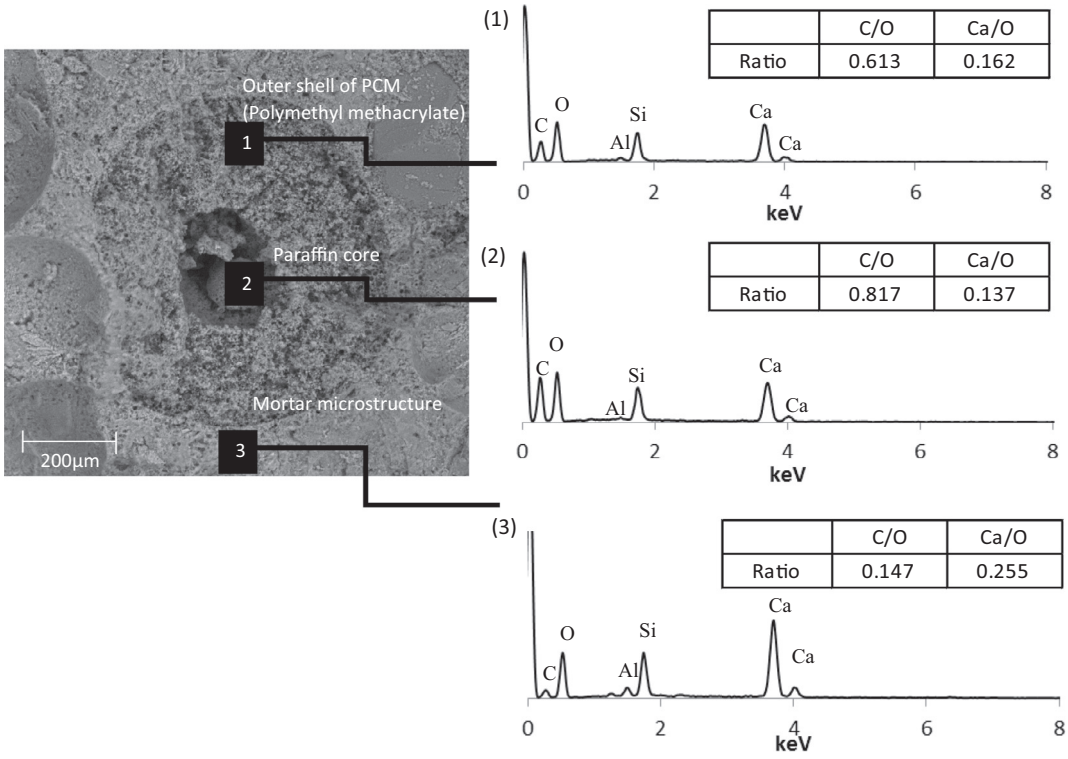

Fig. 17. EDS analysis of SEM micrograph (using BSE detector) of broken PCM particle and its adjacent area.

propagation across the spherical voids of PCM particles and around the aggregate perimeter was noticed on the fracture plane. Essentially, the organic polymer shell of the PCM microcapsule is a soft material compared with the inorganic other constituents in the mix. Thus, during loading of the mortar specimen, PCM particles act as crack initiation point and the fracture will propagate across the weakest point on the matrix which includes the PCM particle and the perimeter of the fine aggregates.

EDS analysis of different areas around a broken PCM microcapsule was carried out and presented in Fig. 17 which includes (1) the broken particles of the polymer shell, (2) the inner core of paraffin, (3) the mortar microstructure. The analysis of the damaged PCM particles confirms the paraffin core with high concentration of Carbon (C) in the centre and high Calcium (Ca) and Silica (Si) concentration in the adjacent mortar microstructure. The calculated chemical composition based on C/O ratio for paraffin core is 0.817 compared to 0.147 on mortar microstructure and 0.613 for outer shell respectively. The Ca/O ratio on mortar microstructure showed highest value of 0.255 compared with 0.137 for the paraffin core.

The elemental mapping of broken PCM particles provides further indication on the graphical distribution of the analysed chemical elements on the micrograph [29]. As in Fig. 18, high concentration of C can be found in the exposed middle area of

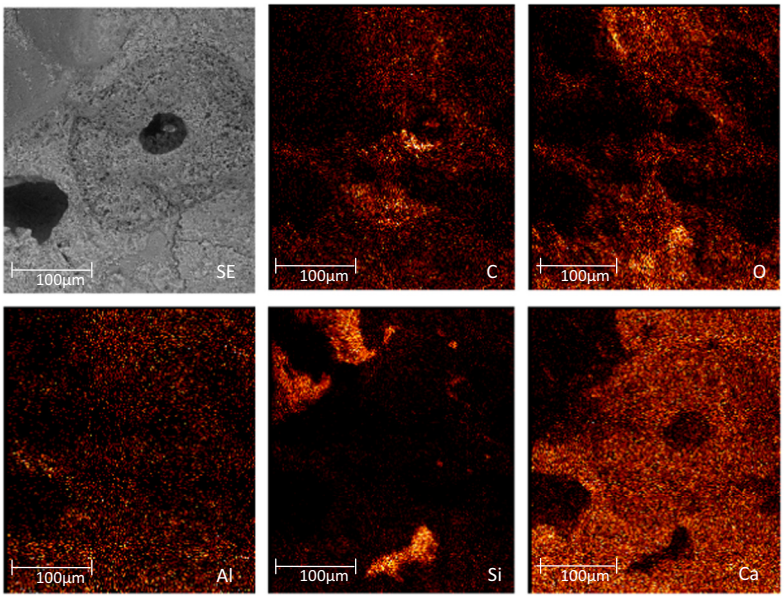

Fig. 18. EDS elemental mapping of failed PCM particle with C, O, Ca, Si and Al elemental distribution maps.

PCM particle which is the paraffin core. Some evidence of leaked wax on the surface, adjacent to the perimeter of the PCM microcapsules was noticed on the C map. This indicates that the damage to the PCM particle was most probable during loading where leaked paraffin wax accumulates around the PCM particle rather than open pores. The elemental distribution map on Ca shows high concentration and continuous distribution across the PCM particle to the adjacent binder thus indicates that PCM particle is well bonded in the structure. The less concentrated area of Ca was observed on the open pores and the exposed middle area of PCM that relates to inner paraffin core with high concentration of C as shown in Fig. 17.

4. Conclusions

Microencapsulated PCM substituted for fine aggregates in cementitious mortar and concrete was used to improve the thermal performance of the material. This study showed that as the volume fraction of PCM in substitution was increased, the thermal conductivity and diffusivity was decreased while the heat capacity was increased. However a loss of strength due to substitution can be a drawback. Even if the fineness of the PCM involves a filler effect and increases the cement hydration, its low density compared with the fine aggregates decreased the strength by 27% per 20% of PCM in volume substitution. As microencapsulated PCM particles are the weakest component of the specimen due to their polymeric nature, developing a stronger outer shell PCM could be a solution. Moreover contrary to most of previous findings, microscopic analysis showed that micronised PCM particles were strongly bonded to the binder and not damaged during mixing. With regards to all the results derived in this study it is concluded that 20% replacement is found to be the optimum level of microencapsulated PCM in cementitious mortar and concrete with acceptable level of strength for most of the structural and non-structural purposes, and provides significant benefits on thermal performance for reduction of heating and cooling loads in buildings.

Acknowledgements

This work is supported by APA, Australian Postgraduate Award offered from the University of Melbourne, Australia. The authors acknowledge the generous provision of materials from BASF (Australia and New Zealand) and gratefully acknowledge the support from Laura Jukes for the experiments in this study.

References

[1] A. Pasupathy, R. Velraj, R.V. Seeniraj, Phase change material-based building architecture for thermal management in residential and commercial establishments, Renew. Sustain. Energy Rev. 12 (1) (2008) 39–64.
[2] D.P. Bentz, R. Turpin, Potential applications of phase change materials in concrete technology, Cem. Concr. Compos. 29 (7) (2007) 527–532.
[3] M. Ahmad, A. Bontemps, H. Sallee, D. Quenard, Thermal testing and numerical simulation of a prototype cell using light wallboards coupling vacuum isolation panels and phase change material, Energy Build. 38 (6) (2006) 673–681.
[4] C. Voelker, O. Kornadt, M. Ostry, Temperature reduction due to the application of phase change materials, Energy Build. 40 (5) (2008) 937–944.
[5] P. Schossig, H.M. Henning, S. Gschwander, T. Haussmann, Micro-encapsulated phase-change materials integrated into construction materials, Sol. Energy Mater. Sol. Cells 89 (2–3) (2005) 297–306.
[6] J. Li, P. Xue, W. Ding, J. Han, G. Sun, Micro-encapsulated paraffin/high-density polyethylene/wood flour composite as form-stable phase change material for thermal energy storage, Sol. Energy Mater. Sol. Cells 93 (10) (2009) 1761–1767.
[7] L.F. Cabeza, C. Castellon, M. Nogues, M. Medrano, R. Leppers, O. Zubillaga, Use of microencapsulated PCM in concrete walls for energy savings, Energy Build. 39 (2) (2007) 113–119.
[8] A.G. Entrop, H.J.H. Brouwers, A.H.M.E. Reinders, Experimental research on the use of micro-encapsulated Phase Change Materials to store solar energy in concrete floors and to save energy in Dutch houses, Sol. Energy 85 (5) (2011) 1007–1020.
[9] M. Hunger, A.G. Entrop, I. Mandilaras, H.J.H. Brouwers, M. Founti, The behavior of self-compacting concrete containing micro-encapsulated phase change materials, Cem. Concr. Compos. 31 (10) (2009) 731–743.
[10] P. Meshgin, Y. Xi, Effect of phase change materials on properties of concrete, ACI Mater. J. 109 (1) (2012) 71–80.
[11] P.K. Dehdezi, M.R. Hall, A.R. Dawson, S.P. Casey, Thermal, mechanical and microstructural analysis of concrete containing microencapsulated phase change materials, Int. J. Pavement Eng. 14 (5) (2013) 449–462.
[12] ASHRAE Handbook – Fundamentals, American Society of Heating, Refrigerating and Air-Conditioning Engineers Inc., Atlanta, GA, 2013.
[13] F. Fernandes, S. Manari, M. Aguayo, K. Santos, T. Oey, Z. Wei, et al., On the feasibility of using phase change materials (PCMs) to mitigate thermal cracking in cementitious materials, Cem. Concr. Compos. 51 (2014) 14–26.
[14] AS 3972 General Purpose and Blended Cements, Standards Australia, 2010.
[15] AS 2350.2 Methods of Testing Portland, Blended and Masonry Cements – Method 2: Chemical Composition, Standards Australia, 2006.
[16] AS 1141.11.1 Methods for Sampling and Testing Aggregates - Particle Size Distribution – Sieving Method, Standards Australia, 2011.
[17] AS 1012 3.1 Methods of Testing Concrete; Determination of Properties Related to the Consistency of Concrete – Slump Test, Standards Australia, 2014.
[18] AS 1012.1 Methods of Testing Concrete; Method 1 – Sampling of Concrete, Standards Australia, 2014.
[19] AS 1012.9 Methods of Testing Concrete; Compressive Strength Tests – Concrete, Mortar and Grout Specimens, Standards Australia, 2014.
[20] M. Kheradmand, M. Azenha, J.L.B. de Aguiar, K.J. Krakowiak, Thermal behavior of cement based plastering mortar containing hybrid microencapsulated phase change materials, Energy Build. 84 (2014) 526–536.
[21] ASTM D5334-14 Standard Test Method for Determination of Thermal Conductivity of Soil and Soft Rock by Thermal Needle Probe Procedure, ASTM International, West Conshohocken, PA, 2014.
[22] F.J. Luo, L. He, Z. Pan, W.H. Duan, X.L. Zhao, F. Collins, Effect of very fine particles on workability and strength of concrete made with dune sand, Constr. Build. Mater. 47 (2013) 131–137.
[23] H.S. Yang, Y.J. Che, Influence of particle size distribution of fine and micro-aggregate on the microstructure of cement mortar and paste, Mater. Res. Innovations 19 (2015) S1–S130.
[24] L. Soriano, J. Monzó, M. Bonilla, M.M. Tashima, J. Payá, M.V. Borrachero, Effect of pozzolans on the hydration process of Portland cement cured at low temperatures, Cem. Concr. Compos. 42 (2013) 41–48.
[25] K. De Weerdt, M. Ben Haha, G. Le Saout, K.O. Kjellsen, H. Justnes, B. Lothenbach, Hydration mechanisms of ternary Portland cements containing limestone powder and fly ash, Cem. Concr. Res. 41 (3) (2011) 279–291.
[26] I. Pane, W. Hansen, Investigation of blended cement hydration by isothermal calorimetry and thermal analysis, Cem. Concr. Res. 35 (6) (2005) 1155–1164.
[27] J. Tikkanen, A. Cwirzen, V. Penttala, Effects of mineral powders on hydration process and hydration products in normal strength concrete, Constr. Build. Mater. 72 (2014) 7–14.
[28] M.H.N. Yio, J.C. Phelan, H.S. Wong, N.R. Buenfeld, Determining the slag fraction, water/binder ratio and degree of hydration in hardened cement pastes, Cem. Concr. Res. 56 (2014) 171–181.
[29] M. Vespa, E. Wieland, R. Dähn, D. Grolimund, A.M. Scheidegger, Determination of the elemental distribution and chemical speciation in highly heterogeneous cementitious materials using synchrotron-based micro-spectroscopic techniques, Cem. Concr. Res. 37 (11) (2007) 1473–1482.